

Magnetic resonance of thin-film single-crystal epitaxial dilute alloys*

D. Arbilly and Guy Deutscher

Department of Physics and Astronomy, Tel Aviv University, Ramat Aviv, Tel Aviv, Israel

Enrique Grunbaum

School of Engineering, Tel Aviv University, Ramat Aviv, Tel Aviv, Israel

R. Orbach[†]

Physics Department, University of California, Los Angeles, California 90024

J. T. Suss

Solid State Physics Department, Israel Atomic Energy Commission, Soreq Nuclear Research Center, Yavne 70600, Israel

(Received 21 April 1975)

The magnetic resonance of thin ($< 1 \mu\text{m}$) Ag:Er films, epitaxially grown on cleaved NaCl (001) faces, is reported. An anisotropy associated with the thermal strain is observed. The magnitude of the anisotropy allows for the extraction of the orbit-lattice coupling constant. The angular variation of the linewidth is ascribed to a spatial dependence of the internal strain. It is shown that systematic linewidth studies as a function of film thickness will allow for the extraction of the internal strain distribution for an epitaxially grown film.

I. INTRODUCTION

The remarkable sensitivity of electron-spin resonance (ESR) in metals allows one to use ESR as a spin label. In this paper we demonstrate how one can use ESR to probe the internal strain field, its overall magnitude, direction, and spatial distribution, in an epitaxially grown thin single-crystal film.

We have chosen the system Ag:Er because of its well-characterized magnetic resonance spectrum,¹ and the relatively good epitaxial growth of Ag on a (001) NaCl cleavage face at 280 °C.² We observed magnetic resonance signals for films with thicknesses ranging from 700 Å to over a micron. We operate at nominal Er concentrations of 10 000 ppm, but, as discussed in Sec. II, have reason to believe that the ESR signal concentration is closer to 200 ppm. We analyze our results using the known crystal-field splitting of Ag:Er, and the strain induced by differential thermal contraction at the Ag-NaCl interface. The measured anisotropy of the g factor then enables us to calculate the magnitude of the orbit-lattice coupling constant for a metal. This is the first time that this important coupling strength has been determined.

The ESR linewidth varies as the magnetic field is rotated in a plane perpendicular to the film. The width is maximum when the field is perpendicular to the film, and minimum when the field is along the [111] direction. This is direct evidence for an anelastic falloff of the strain amplitude through the thickness of the film, with the axis perpendicular to the film. One should be able to extract the de-

tailed internal strain-field spatial distribution by analyzing the ESR line shape as a function of film thickness.

In Sec. II, we describe the experimental techniques involved in the thin-film alloy deposition, and the electron-spin-resonance measurements. In Sec. III we discuss the determination of the concentration of Er in the samples, and in Sec. IV we present the basis of our theoretical analysis. Experiment is compared with theory in Sec. V. Our conclusions are presented in Sec. VI, together with a discussion of the prospects for investigating the structure of other epitaxially grown materials.

II. EXPERIMENTAL TECHNIQUES AND RESULTS

A. Sample preparation and structure

A Varian VT-422 ultra-high-vacuum system was used for the preparation of the thin films at a base pressure of 3×10^{-8} Torr. The evaporation of silver doped with an atomic concentration of 1% erbium (prepared by arc melting) was carried out from a tungsten boat onto a (001) surface plane of NaCl crystals freshly cleaved to approximately a thickness of 0.5 mm. In order to achieve single-crystal films of Ag on NaCl with a relatively low defect concentration, the surface of the NaCl was exposed to water vapor.³ The temperature of the NaCl substrate in the vacuum system before evaporation was held at 270 °C and rose during evaporation to 280 °C.^{2,4} The thickness of the deposited film, as well as the deposition rate (5–10 Å/sec), was measured by a QM-11 Kronos thickness monitor. The samples were kept at 270 °C for 1 h after

evaporation and cooled slowly thereafter. After removing the samples from the ultra-high-vacuum system, a 200-Å carbon film was deposited to protect the fresh silver film from corrosion. Care was taken not to expose the films to air for any significant length of time. It was noted that some of the films exposed to air for about an hour exhibited wrinkles on the surface of the film.

Transmission electron diffraction and microscopy, as well as x-ray diffraction, showed that these films were high quality single crystals.

B. ESR measurements

A Varian EC-365 X-band spectrometer was used, with a TE₀₁₂ reflection cavity. The magnetic field supplied by a Varian 6-inch electromagnet was calibrated by a proton resonance magnetometer. The samples were pasted to the cavity on the uncoated (001) NaCl face, and the magnetic field H_{dc} was rotated in the (100) plane.

A typical ESR spectrum of Er in a 7,400 Å film of Ag on a NaCl substrate with H_{dc} along the [011] direction is shown in Fig. 1. The angular variation of the g factor and the linewidth were studied in the (100) plane. The g factors and linewidths were determined according to a procedure outlined in Ref. 5. A computer fit for the g factor

$$g = (g_{\parallel}^2 \cos^2 \theta + g_{\perp}^2 \sin^2 \theta)^{1/2},$$

where θ is the angle between the magnetic field and the z axis (perpendicular to the plane of the film), yielded the following results:

$$g_{\parallel} = g_{[001]} = 6.6346 \pm 0.0046;$$

$$g_{\perp} = g_{[010]} = 6.8886 \pm 0.0046.$$

The absolute error is ± 0.06 . The measured and computed data for the variation of the g factor are shown in Fig. 2. The experimental data points for the linewidths were fitted to

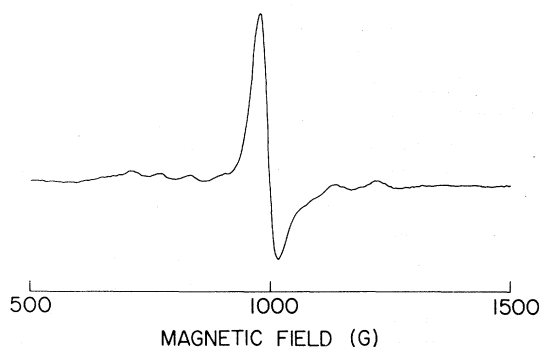


FIG. 1. ESR spectrum of Er in a 7400-Å film of Ag on a NaCl substrate, at 1.6 K and 9.38 GHz. H_{dc} is along the [011] direction. The hyperfine structure because of ^{167}Er is resolved.

$$\Delta H_{1w} = a + b |3 \cos^2 \theta - 1|,$$

(see Sec. V) with the following values for a and b :

$$a = 35.2 \pm 0.65\text{G}; \quad b = 4.0 \pm 0.55\text{G}.$$

The measured and computed variation of the linewidth are exhibited in Fig. 3.

III. DETERMINATION OF THE ER CONCENTRATION IN THE FILMS

The concentration of Er was determined by: (a) measuring the residual resistance of single-crystal silver films prepared simultaneously with the ESR sample but evaporated onto mica substrates at 270°C using a suitable mask for four-terminal measurement, and (b) by measuring the relative intensity of the electron-spin-resonance signal. The resistance was measured at room, liquid-nitrogen, and liquid-helium temperatures. The residual resistivity of a normal conductor containing a small concentration of an impurity can be written

$$\rho = \rho_0 + kc, \quad (1)$$

where ρ_0 is the residual resistance of the "pure" conductor, and c the impurity concentration. Using resistivity data for bulk Ag containing 1 at. % of ^{77}Er and for pure bulk Ag,⁸ one obtains a value of $k = 6 \times 10^{-4} \mu\Omega \text{ cm}$ per ppm of Er in Ag. We found from the measured resistivity of the 7400-Å sample, using Eq. (1) and the above value for k , that the

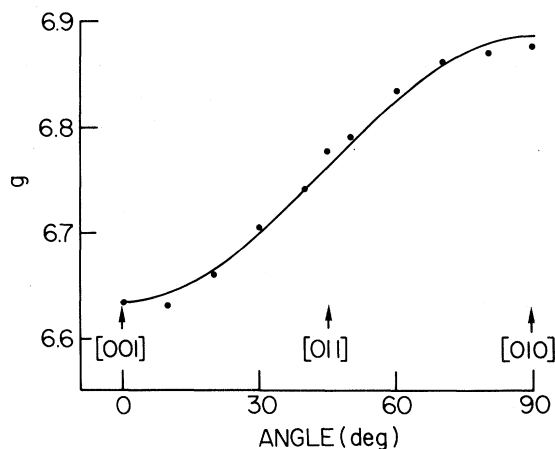


FIG. 2. Angular variation of the g factor of Er in a 7400-Å film of Ag on a NaCl substrate at 1.6 K and 9.38 GHz. H_{dc} was rotated in the (100) plane. The solid curve represents a best fit of the experimental data points to: $(g_{\parallel}^2 \cos^2 \theta + g_{\perp}^2 \sin^2 \theta)^{1/2}$. Here θ is the angle between the magnetic field H_{dc} and the z axis (perpendicular to the plane of the film). Thus, g_{\parallel} corresponds to $\theta = 0$ and H_{dc} perpendicular to the plane of the film along the [001] direction, g_{\perp} corresponds to $\theta = 90^\circ$ and H_{dc} in the plane of the film along the [010] direction. The g factors were determined according to a procedure outlined in Ref. 5.

Er concentration was 200 ppm. The error in this estimate is less than 10%. The ESR signal intensity (measured relative to a standard) was consistent with this value.

The large difference between the film Er concentration, and that of the source material, is undoubtedly associated with the difference in vapor pressure between Ag and Er (the former is an order of magnitude larger than the latter at the temperature of the single tungsten boat⁹). The source material was evaporated to completion, and the "missing" Er may have been absorbed by the tungsten boat.

There is no evidence for large concentration gradients. The measured ESR resonance peaks exhibited an asymmetry¹⁰ indicating that the spins contributing to the signal lie within the skin depth (estimated to be 1900 Å for the 7400-Å sample).

Finally, the fact that we were able to resolve the hyperfine splitting so clearly (see Fig. 1) implies that the magnetically active Er impurities must be at effective local concentrations less than 500 ppm [see Ref. 1, Phys. Rev. B **2**, 2298 (1970)].

IV. THEORETICAL FRAMEWORK

A. Strains in the film and anisotropy in the g factor

Experiments in which external stresses are applied to thin films, especially to crystalline single films, show that they possess very high tensile strengths. Pure elastic behavior occurs¹¹ for strains as high as from 1 to 5%. In addition, the elastic moduli are found to differ only slightly from those of the bulk material.¹¹ In view of these results, the calculated thermal strains at the in-

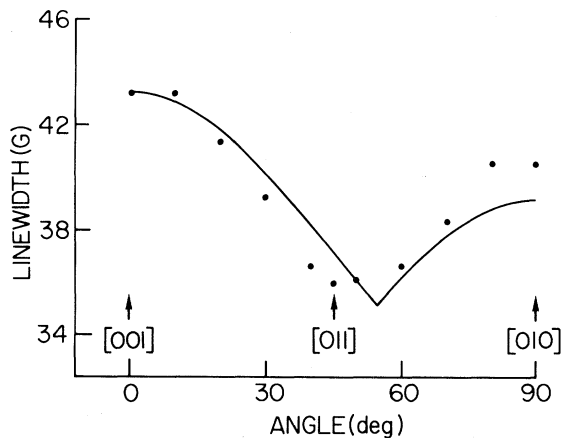


FIG. 3. Angular variation of the linewidth of Er in a 7400-Å film of Ag on a NaCl substrate. Experimental conditions are the same as in Fig. 2. The solid curve here represents a best fit of the experimental data points to: $a + b|3 \cos^2 \theta - 1|$. The linewidths were determined according to a procedure outlined in Ref. 5.

terface of our samples could be smaller than the elastic limit of the films.

The films were deposited at 280 °C (see Sec. II) and their ESR spectrum measured at helium temperatures. Contraction of both film and substrate takes place between deposition and measurement temperatures. Because the contraction of an alkali halide is larger than that of the metal, the NaCl substrate will apply a compressive stress to the film at the interface, parallel to its plane. If the bonding between the Ag film and the NaCl interface is sufficiently strong, a planar contraction of the Ag lattice constant at the interface plane, with a concomitant expansion of the lattice cell perpendicular to this direction, is expected. Labeling the latter direction as the z axis, one can identify the interface strains,

$$e_{xx} = e_{yy} = \int_{T_m}^{T_d} (\alpha_{Ag} - \alpha_{NaCl}) dT = -1.07\%, \quad (2)$$

where α_{Ag} , α_{NaCl} are the coefficients of thermal expansion of Ag, and NaCl, respectively, and both are temperature dependent.¹² The temperature of the substrate during the deposition T_d equaled 553 K, while $T_m = 1.6$ K is the temperature during the ESR measurements. The variation of α_{Ag} and α_{NaCl} with temperature was taken into account in arriving at the value of the interface strain in Eq. (2). Elasticity theory requires

$$e_{zz} = \left| -\nu/(1-\nu) \right| (e_{xx} + e_{yy}) = 1.61\%, \quad (3)$$

where ν is Poisson's ratio, equal¹² to 0.43 for bulk single crystalline Ag. If these strains were uniform throughout the film, the volume contraction would be

$$e_{xx} + e_{yy} + e_{zz} = 2e_{xx}(1-2\nu)/(1-\nu) = -1.07\% - 1.07\% + 1.61\% = -0.53\%. \quad (4)$$

This volume change, though significant, will not affect our estimate of the spin phonon coupling constant (see discussion in Sec. V).

Let the interface planes be denoted by the coordinate $z = 0$, with film occupying $0 \leq z \leq d$ (d is the film thickness). As z increases, one would normally not expect the strain to change for a thin film on a thick substrate, where the lateral dimensions of the film greatly exceed the film thickness.¹³ This conclusion holds only while in the elastic regime. We shall see below that evidence is present in our measurements for a spatial distribution of strain in the film, leading to the conclusion that some anelastic behavior is present. Because the thermal strain is small [see Eq. (2)], one can use perturbation theory for the g tensor in uniaxially strained materials

$$g_{||} + 2g_{\perp} = 3g, \quad (5)$$

where g is the isotropic value for the unstrained cubic crystal. Here, \parallel and \perp refer to the magnetic field perpendicular and parallel to the plane of the film, respectively. For Ag:Er, the ground doublet is a Γ_7 , with a g value equal to 6.7968.^{1,14} The first excited state is thought¹⁴ to lie at 35 K, and to be of $\Gamma_8^{(1)}$ character (in the notation of Lea *et al.*¹⁵). The angular variation of the g factor can be determined using Eq. (5). We define $\Delta g_{\parallel} = g_{\parallel} - g$ (so that $\Delta g_{\perp} = -2\Delta g_{\parallel}$). To first order,

$$g(\theta) = (g_{\parallel}^2 \cos^2 \theta + g_{\perp}^2 \sin^2 \theta)^{1/2} \\ \cong g + \frac{1}{2} \Delta g_{\parallel} (3 \cos^2 \theta - 1), \quad (6)$$

where θ is the angle between the magnetic field and the z axis (perpendicular to the plane of the film). Thus, measurement of $g(\theta)$ gives an immediate test of the model. It will yield the uniaxially undistorted g value (along the [111] direction where $\cos^2 \theta = \frac{1}{3}$), and provides a direct measure of Δg_{\parallel} . Knowledge of the crystal-field level positions of Ag:Er then allows one to evaluate the strength of the distortion mixing of the Er wave functions, and from this the orbit-lattice interaction.¹⁶

B. Strain distribution in the film and anisotropy in the ESR linewidth

Before considering the crystal-field mixing expression, we note that if the strain is not constant across the film, the ESR linewidth will increase because of the spatial distribution of g values. One can see this directly from Eq. (6) if Δg_{\parallel} is allowed to be a function of z . The measured $g(\theta)$ then

$$P_{\text{obs}}(H) = \sum_{z=0}^{z=n} \frac{T_2/\pi}{1 + (\gamma T_2)^2 [H - [H_0 + \Delta H(z)]]^2} \\ = \sum_{z=0}^{z=n} \frac{T_2/\pi}{1 + (\gamma T_2)^2 [H - H_0 [1 - \frac{1}{2} F(z) (\Delta g_{\parallel}/g) (3 \cos^2 \theta - 1)]]^2}, \quad (10)$$

where n is twice the number of lattice constants making up the thickness of the film. One usually observes¹⁰ the field derivative of Eq. (10) in equal combination with the dispersive signal in thick samples. In thin films, the combination will be different but can be extracted from the line shape. As can be seen from Eq. (10), the linewidth diminishes to a minimum at $\cos^2 \theta = \frac{1}{3}$ [the (111) direction], where it assumes its strain-free value. As described in Sec. II, the g value and linewidth along the [111] direction behave as observed in the bulk,¹ and demonstrate crystal quality as good as any bulk crystals yet fabricated.

The form of the line shape in Eq. (10) is not symmetrical. The sense of the asymmetry depends on the sign of Δg_{\parallel} and the angle θ . Epitaxially grown Ag:Er on NaCl has $\Delta g_{\parallel} < 0$ (Sec. II). For $\theta = 0$, the line is shifted to higher fields, and is therefore

represents a spatial average over the film

$$g(\theta) = \frac{1}{d} \int_0^d g(\theta, z) dz,$$

where $g(\theta, z)$ represents Eq. (6) evaluated at the position z where the strain has the value $\epsilon_{\alpha\alpha}(z)$. Defining the average strain

$$\bar{\epsilon}_{\alpha\alpha} = \frac{1}{d} \int_0^d \epsilon_{\alpha\alpha}(z) dz,$$

we may introduce a strain distribution function $F(z) = \epsilon_{\alpha\alpha}(z) / \bar{\epsilon}_{\alpha\alpha}$. Clearly, $F(z) > 1$ for $z \approx 0$ (at the interface), and $F(z) \leq 1$ for $z \approx d$ (at the film's free surface). Then, in an obvious notation,

$$g(\theta, z) = g + \frac{1}{2} F(z) \Delta g_{\parallel} (3 \cos^2 \theta - 1). \quad (7)$$

If we measured z in units of half the lattice constant (for a fcc lattice), the field for resonance, H_{res} , will be shifted from its unperturbed value H_0 by

$$\Delta H(z) = H_{\text{res}}(z) - H_0 = - (H_0/g) [g(\theta, z) - g] \\ = - \frac{1}{2} H_0 F(z) (\Delta g_{\parallel}/g) (3 \cos^2 \theta - 1). \quad (8)$$

If the unstrained absorption line shape is Lorentzian, the power absorbed will be proportional to¹⁷

$$P(H) = \frac{T_2/\pi}{1 + \gamma^2 T_2^2 (H - H_{\text{res}})^2}, \quad (9)$$

where T_2 is the transverse relaxation time, and $\gamma = g \mu_B / \hbar$. Because H_{res} is a function of z , the observed line shape will be given by the sum

broader on the low-field side. For $\theta > 54.7^\circ$, the line is broader on the high-field side. This is because the g value is shifted maximally at $\theta = 0$, $z = 0$. As z increases, $F(z)$ diminishes, and the field for resonance diminishes (because $\Delta g_{\parallel} < 0$). The anelastic strain-induced width is large, and the spatial variation of the g value the largest, if n in Eq. (10) is modest [i.e., $F(z=n) \approx 1$]. On the contrary, for thick films [$F(z=n) \ll 1$] there is almost no thermal strain-induced width, and the g value hardly departs from the [111] value. Thus, measurements of the resonance characteristics as a function of film thickness can yield a direct measure of the anelastic strain, and its "healing length." Careful measurements, utilizing detailed models for $F(z)$ in Eq. (10), can yield the actual internal strain-field distribution. To our knowledge,

no other method exists which can generate such detailed information.

C. Determination of the orbit-lattice coupling constant

Finally, knowledge of Δg_{\parallel} can yield information regarding the sign and magnitude of the axial orbit-lattice coupling constant. According to Blume and Orbach,¹⁸

$$V_{\text{OL}} = \sum_{i, l, m} V(\Gamma_{ig} l) C(\Gamma_{ig} m, l) e(\Gamma_{ig}, -m) (-1)^m. \quad (11)$$

Here, i stands for the irreducible representation of the cubic group, with m a particular subvector. $V(\Gamma_{ig} l)$ is the orbit-lattice coupling coefficient, where $l=2, 4$, or 6 for rare earths. $C(\Gamma_{ig} m, l)$ is the appropriate combination¹⁶ of spherical harmonics acting on the $4f$ electron coordinates, while $e(\Gamma_{ig}, m)$ is the appropriate linear combination¹⁶ of phonon strain amplitudes. We need only consider $i=3$, and $m=\theta$ for our case, because the strain is tetragonal: $e_{xx}=e_{yy} \neq e_{zz}$ [$(-1)^\theta$ is defined as unity]. Evaluating $e(\Gamma_{3g}, \theta)$ from Eqs. (2) and (3), we find at the interface,

$$e(\Gamma_{3g}, \theta) = \frac{1}{2}(2e_{zz} - e_{xx} - e_{yy}) \\ = \frac{1}{2}(2 \times 1.61 + 1.07 + 1.07)\% = 2.68\%. \quad (12)$$

We have, however, three terms in Eq. (11) to evaluate, appropriate to $l=2, 4$, or 6 . We have no way of separating these terms. For simplicity (there will be some justification for this procedure in Sec. V) we drop the $l=4$ and 6 terms so that

$$V_{\text{OL}} = V(\Gamma_{3g} 2) C(\Gamma_{3g} \theta, 2) \frac{1}{2}(2e_{zz} - e_{xx} - e_{yy}). \quad (13)$$

We use Eq. (13) to mix the first excited state $\Gamma_8^{(1)}$ into the ground Γ_7 , utilizing the wave functions for Er appropriate to Williams and Hirst's values¹⁴ for x and W (-0.338 and 0.555 K, respectively) in the notation of Lea *et al.*¹⁵ for the unperturbed wave functions and eigenvalues. These parameters lead to a first excited level of Γ_8 character, some 35 K higher in energy than the ground level. A Γ_6 lies at 40 K, with the remaining two Γ_8 's near 200 K. Only the Γ_8 are connected to the ground Γ_7 by Eq. (13). To an accuracy of $\approx 10\%$, this means we need only include the lower lying $\Gamma_8^{(1)}$ in our analysis. A more detailed calculation is straightforward but unwarranted at the present time. Any volume expansion would alter x and W , but the Γ_7 g factor remains the same because $g(\Gamma_7)$ is independent of x and W . Mixing the excited $\Gamma_8^{(1)}$ into the ground Γ_7 with Eq. (13) shifts the g value. Using Eq. (13), the measured shift allows us to extract $V(\Gamma_{3g} 2)$. Explicitly,

$$\frac{\Delta g_{\parallel}}{g} = - \frac{0.0156 V(\Gamma_{3g} 2) \frac{1}{2}(2e_{zz} - e_{xx} - e_{yy})}{6.7968}, \quad (14)$$

where the numerical coefficient in the numerator arises from explicit matrix elements of $C(\Gamma_{3g} \theta, 2)$ between Γ_7 ground state and the ($x=0.338$) excited $\Gamma_8^{(1)}$ state, divided by the splitting to the latter of 34.8 K. The denominator is the g factor of the Γ_7 ground state. As we shall see in Sec. V, the numerical value for $V(\Gamma_{3g} 2)$ is comparable to the cubic crystalline field coefficients for Er in Ag (as noted by Orbach¹⁹ previously for insulators), but smaller in magnitude than in insulators.

V. COMPARISON OF THEORY AND EXPERIMENT

The experimental results of Sec. II yield

$$\Delta g_{\parallel}/g = -0.0249. \quad (15)$$

From Eq. (14) this leads to

$$V(\Gamma_{3g} 2) \frac{1}{2}(2e_{zz} - e_{xx} - e_{yy}) = 10.8 \text{ K}. \quad (16)$$

To our knowledge, this is the first quantitative estimate of the orbit-lattice coupling constant in a metal. It is interesting to compare Eq. (16) with the Williams and Hirst values for the (unstrained) cubic-crystalline-field parameters¹⁴:

$$C_4 = -70.4 \text{ K}, \quad C_6 = 12.8 \text{ K}. \quad (17)$$

Comparing Eq. (17) with Eq. (16) supports the phenomenological concept, previously applied to insulating hosts,¹⁹ that the orbit-lattice coupling constant at unit strain approximates the static crystalline field coupling constant. It should also be noted that Eq. (16) is about an order of magnitude smaller than found for insulator hosts (Sroubek *et al.*²⁰ extract an equivalent coefficient for Yb^{3+} in ThO_2 of ~ 100 K). Inserting the known value of thermal strain at the interface [Eq. (2) into Eq. (16)], we obtain²¹

$$V(\Gamma_{3g} 2) \geq 403.0 \text{ K}. \quad (18)$$

As indicated in Sec. IV, the $l=4$ and 6 terms also contribute. We have omitted them from our parameterization of V_{OL} . It is shown in Sroubek *et al.*²⁰ that these terms are small in insulating hosts when compared to the $l=2$ term, both for point-charge and point dipole models. This may not be relevant to metallic hosts, because of screening of long-range charge contributions to V_{OL} , which diminish the $l=2$ terms compared to the $l=4$ and 6 terms (the former falling off as $1/R^3$, the latter as $1/R^5$ and $1/R^7$, respectively). However, impurity screening, arising from the p -like virtual bound-state electrons, can contribute to the axial potential and may over come this reduction, restoring the validity of our truncation procedure. The p electrons do not contribute to $l=4$ or $l=6$ terms in V_{OL} .

The angular variation of the linewidth follows

from the variation of the factor

$$\left(\frac{1}{2}H_0\right)F(z)(\Delta g_{||}/g)(3 \cos^2\theta - 1)$$

with z in Eq. (10). Experimental results are exhibited in Fig. 3. Fitting to

$$\Delta H_{1w} = a + b |3 \cos^2\theta - 1| \quad (19)$$

gives a best fit of

$$a = 35.2 \pm 0.65 \text{ G}; \quad b = 4.0 \pm 0.55 \text{ G}. \quad (20)$$

The interpretation of Eq. (20) is not trivial. The linewidth coefficient γT_2 in Eq. (10) must be field dependent because, at 1.6 K, only 14 G of the measured linewidth can be attributed to homogeneous broadening.¹ The remainder is associated with an inhomogeneous broadening which manifests itself through an isotropic spread in g values. Because the field for resonance is anisotropic, this spread will yield a variation of linewidth with angle. However, the maximum variation caused by this artifact is less than 1 G. In any case, the observed variation of linewidth for angles between the [011] and [010] directions is contrary to that which would have resulted from the angular variation of field for resonance. The measured linewidth increases, whereas the field for resonance decreases in that angular range. Thus, the predominant contribution to the angular variation arises from the spatial dependence of the thermal strain caused by anelastic behavior. The fit to Eq. (19) exhibited in Fig. 3 is not very good. This is most probably caused by the fact that Eq. (19) is an approximation. One must compute the actual line shape given by Eq. (10) with a trial $F(z)$ in order to establish an effective linewidth at any angle θ .

The fact that this contribution to the linewidth is substantially less than the shift in resonance field with angle (~ 250 G) indicates a relatively small region of anelastic behavior for Ag:Er on NaCl. The actual range of anelastic strain may be larger than a direct application of Eq. (10) would indicate because the signal from spins at the interface is reduced by the skin effect (see Ref. 17). Further experiments must be performed on films of varying thicknesses to allow a quantitative analysis. In any case, we have shown that the angular behavior of the magnetic resonance linewidth can be used to extract the spatial variation of the internal strain distribution in an epitaxially grown thin

film. Indeed, once the orbit-lattice coupling constant has been determined for a particular impurity in a specific host, the measured g shift can be used to obtain the absolute magnitude of the thermal strain distribution in the epitaxial film.

VI. CONCLUSIONS

This paper has presented the first observation and analysis of ESR in epitaxially grown thin metallic films. The presence of the thermal strain results in an anisotropic g factor, and an anisotropic linewidth. The former allows for the extraction of the orbit-lattice coupling constant, the latter an estimate of the magnitude and spatial dependence of the anelastic response.

For the future, it is important that further measurements be made for a variety of film thicknesses. As discussed in Sec. IV, this will enable one to extract the range and shape of the internal strain-field distribution. This may have important consequences for a variety of epitaxially grown materials. The sensitivity of electron-paramagnetic resonance (EPR) is sufficient to dope almost any material at such low impurity concentration levels that the material characteristics are not altered, and the magnetic impurities do not interfere with one another. The magnetic impurity acts as a spin label, and serves as a sensitive probe of the internal strain distribution. By variation of film thickness, one could determine the range of the thermal strain distribution, and thereby the optimum film thickness for a material in question, depending on design considerations. Portis²² has even suggested that ESR in epitaxial films could be used as a microscopic "strain gauge," capable of measuring substrate deformations caused by phase transitions, etc. Though the technique is in its infancy, it seems apparent to the authors that its prospects for materials characterization are great.

ACKNOWLEDGMENTS

The authors wish to acknowledge valuable discussions with Dr. R. J. Wasilewski, and the advice of Dr. Don Thompson and Professor Stanley Dong concerning the boundary-value problem of a thin film on a thick substrate.

*Supported in part by the National Science Foundation and the U. S. Office of Naval Research.

†Support is gratefully acknowledged from the John Simon Guggenheim Memorial Foundation in the form

of a one-year fellowship grant, during which part of this work was done.

¹D. Griffiths and B. R. Coles, Phys. Rev. Lett. **16**, 1093 (1966); L. L. Hirst, G. Williams, D. Griffiths, and

- B. R. Coles, *J. Appl. Phys.* **39**, 844 (1968); R. Chui, R. Orbach, and B. Gehman, *Phys. Rev. B* **2**, 2298 (1970); R. Chui, R. Orbach, and B. Gehman, *J. Phys. (Paris)* **32**, C1-909 (1971).
- ²E. Grünbaum, *Vacuum* **24**, 153 (1974).
- ³T. J. Schober, *J. Appl. Phys.* **40**, 4658 (1969).
- ⁴S. Ino, D. Watanabe, and S. Ogawa, *J. Phys. Soc. Jpn.* **19**, 881 (1964).
- ⁵M. Peter, D. Shaltiel, J. H. Wernick, H. J. Williams, J. B. Mock, and R. C. Sherwood, *Phys. Rev.* **126**, 1395 (1962).
- ⁶D. W. Pashley, *Philos. Mag.* **4**, 316 (1959).
- ⁷H. Thomas, S. Levgold, G. de Vries, and J. Bijvoet, *J. Appl. Phys.* **39**, 797 (1968).
- ⁸D. C. Larson and B. T. Boiko, *Appl. Phys. Lett.* **5**, 155 (1964).
- ⁹R. E. Honig, *RCA Rev.* **23**, 567 (1962).
- ¹⁰R. E. Norberg, *Phys. Rev.* **86**, 745 (1952); N. Bloembergen, *J. Appl. Phys.* **23**, 1383 (1952); F. J. Dyson, *Phys. Rev.* **98**, 349 (1955); G. Feher and A. F. Kip, *ibid.* **98**, 377 (1955).
- ¹¹D. W. Pashley, *Proc. R. Soc. Lond. A* **255**, 218 (1960).
- ¹²Dwight E. Gray, *American Handbook of Physics*, 2nd ed. (McGraw-Hill, New York, 1963), pp. 4-17 and 4-74. ν was calculated from the values of S_{11} and S_{12} given on p. 2-51.
- ¹³The authors are indebted to Professor Stanley Dong for assistance with this boundary-value problem.
- ¹⁴G. Williams and L. L. Hirst, *Phys. Rev.* **185**, 407 (1969); and Ref. 1.
- ¹⁵M. R. Lea, M. J. M. Leask, and W. P. Wolf, *J. Phys. Chem. Solids* **23**, 1381 (1962).
- ¹⁶R. Orbach and J. H. Stapleton, in *Electron Paramagnetic Resonance*, edited by S. Geschwind (Plenum, New York-London, 1972), p. 121.
- ¹⁷This result assumes that the skin depth is much larger than the film thickness. In our case, the latter is approximately four times the former, so that the signal from the region of maximum strain will be diminished by roughly a factor of 50 from the signal arising from the spins at the free surface of the film. A complete analysis would have to fold in the spatial dependence of the electromagnetic field (signal strength) with the spatial dependence of the g value.
- ¹⁸M. Blume and R. Orbach, *Phys. Rev.* **127**, 1587 (1962).
- ¹⁹R. Orbach, *Proc. R. Soc. Lond. A* **264**, 458 (1961).
- ²⁰Z. Sroubek, M. Tachiki, P. H. Zimmerman, and R. Orbach, *Phys. Rev.* **165**, 435 (1968).
- ²¹Because the average strain throughout the film is less than the interface value, Eq. (18) represents only a lower limit for the orbit-lattice coupling constant. Only when the magnitude of the anelastic strain "release" has been estimated, the procedure for which is described in Sec. V, can the average strain in the film be determined.
- ²²A. M. Portis (private communication).